Atmos. Chem. Phys., 12, 1051–1066, 2012
www.atmos-chem-phys.net/12/1051/2012/
doi:10.5194/acp-12-1051-2012


Atmospheric Chemistry and Physics

# Polar-night $O_3$, $NO_2$ and $NO_3$ distributions during sudden stratospheric warmings in 2003–2008 as seen by GOMOS/Envisat

**V. F. Sofieva[1], N. Kalakoski[1], P. T. Verronen[1], S.-M. Päivärinta[1,2], E. Kyrölä[1], L. Backman[1], and J. Tamminen[1]**

[1]Finnish Meteorological Institute, Helsinki, Finland
[2]Department of Physics, University of Helsinki, Helsinki, Finland

*Correspondence to:* V. F. Sofieva (viktoria.sofieva@fmi.fi)

Received: 12 July 2011 – Published in Atmos. Chem. Phys. Discuss.: 18 August 2011
Revised: 24 November 2011 – Accepted: 10 January 2012 – Published: 24 January 2012

**Abstract.** Sudden stratospheric warmings (SSW) are large-scale transient events, which have a profound effect on the Northern Hemisphere stratospheric circulation in winter. During the SSW events the temperature in stratosphere increases by several tens of Kelvins and zonal winds decelerate or reverse in direction. Changes in temperature and dynamics significantly affect the chemical composition of the middle atmosphere.

In this paper, the response of the middle-atmosphere trace gases during several sudden stratospheric warmings in 2003–2008 is investigated using measurements from the GOMOS (Global Ozone Monitoring by Occultation of Stars) instrument on board the Envisat satellite. We have analyzed spatial and temporal changes of $NO_2$ and $NO_3$ in the stratosphere, and of ozone in the whole middle atmosphere. To facilitate our analyses, we have used the temperature profiles data from the MLS (Microwave Limb Sounder) instrument on board the Aura satellite, as well as simulations by the FinROSE chemistry-transport model and the Sodankylä Ion and Neutral Chemistry model (SIC). $NO_3$ observations in the polar winter stratosphere during SSWs are reported for the first time.

Changes in chemical composition are found not to be restricted to the stratosphere, but to extend to mesosphere and lower thermosphere. They often exhibit a complicated structure, because the distribution of trace gases is affected by changes in both chemistry and dynamics. The tertiary ozone maximum in the mesosphere often disappears with the onset of SSW, probably because of strong mixing processes. The strong horizontal mixing with outside-vortex air is well observed also in $NO_2$ data, especially in cases of enhanced $NO_2$ inside the polar vortex before SSW. Almost in all of the considered events, ozone near the secondary maximum decreases with onset of SSW. In both experimental data and FinROSE modelling, ozone changes are positively correlated with temperature changes in the lower stratosphere in the dynamically controlled region below ∼35 km, and they are negatively correlated with temperature in the upper stratosphere (altitudes 35–50 km), where chemical processes play a significant role. Large enhancements of stratospheric $NO_3$, which strongly correlate with temperature enhancements, are observed for all SSWs, as expected by the current understanding of temperature-dependence of $NO_3$ concentrations and simulations with the CTM.

## 1 Introduction

Sudden Stratospheric Warmings (SSWs) are large scale perturbing events in the winter polar regions that affect the structure and circulation of the middle atmosphere. SSWs are caused by dissipation of planetary waves, which are generated in the troposphere, in the upper stratosphere (Holton, 2004; Matsuno, 1971; Schoeberl, 1978). This explains, in particular, the fact that sudden stratospheric warmings are rare in the Southern Hemisphere, which is affected much less by planetary waves than the Northern Hemisphere. During a SSW, the zonal mean temperature in polar stratosphere increases by several tens of Kelvins in few days. The warming is accompanied with a weakening of zonal winds and disturbance of the polar vortex. In case of major sudden stratospheric warming, the zonal mean wind is reversed and the polar vortex can break down completely.

It is known since the work of Matsuno (1971) that SSWs are accompanied with a cooling in the mesosphere. This was explained in his paper as a result of the mean flow and planetary wave interaction based on mass balance. Holton (1983) pointed out that the changes in the mean wind profile alter the conditions for the gravity wave propagation and result in reduced gravity wave momentum flux in the mesosphere, which leads to mesospheric cooling

via reducing wave-induced diabatic descent (Garcia and Boville, 1994). SSWs can also have a significant effect on tropospheric weather patterns (Baldwin and Dunkerton, 2001).

The dynamical changes related to SSWs are accompanied by remarkable changes in the chemical composition of the middle atmosphere. First observational case studies were performed already over 30 year ago using in situ (Dutsch and Braun, 1980) and SAGE I satellite measurements (Wang et al., 1983); they have been focused on the stratosphere. The changes in the chemical composition have attracted increasing attention during the last decade because of several reasons. First, observations of trace gases and temperature in the middle atmosphere have become available with several new satellite instruments having good global coverage of polar regions in winter. Second, these observations provide a dataset for testing chemistry-climate models. The response of the middle atmosphere to SSWs is still difficult to simulate (Salmi et al., 2011; Siskind et al., 2010). Third, it has been recently discovered that some of the sudden stratospheric warmings (as observed in 2004 and then again in 2006 and 2009) result in unusual subsequent features: dramatic cooling at $\sim$50 km, then the reformation of stratopause near 80 km, following by the enhanced downward transport from the mesosphere and thermosphere into the polar vortex area. The strong descent of $NO_x$ species is of further interest because it can cause ozone depletion through catalytic chemical reaction cycles. Observational evidences of enhanced downward transport of trace species have been reported in several papers (Damiani et al., 2010; Funke et al., 2005; Hauchecorne et al., 2007; Manney et al., 2008, 2005; Randall et al., 2006, 2009; Renard et al., 2009; Smith et al., 2009; Sofieva et al., 2009).

The short-term changes in stratospheric ozone in response to SSWs have been rather extensively studied using ground-based, in situ and satellite observations (Di Biagio et al., 2010; Dutsch and Braun, 1980; Flury et al., 2009; Kleinböhl et al., 2005; Liu et al., 2009, 2011; Wang et al., 1983). These studies have shown a complicated coupling of chemistry and dynamics and pointed out on necessity of considering evolution of 3-D fields. There are also numerous studies related to the sudden stratospheric warming in the Southern Hemisphere in 2002 (e.g., (Glatthor et al., 2005; Ricaud et al., 2005; Richter et al., 2005), the special issue of Journal of Atmospheric Sciences, Volume 62, Issue 3 (March 2005)).

The short-term changes in the chemical composition of the mesosphere in response to SSWs have been less reported. The experimental studies include observations of OH, ozone and temperature by Microwave Limb Sounder (MLS) in 2005–2009 at altitudes 50–90 km (Damiani et al., 2010), and MLS observations of CO, $N_2O$ and $H_2O$ during SSW in 2009 (Manney et al., 2009).

The response of the middle atmosphere composition to sudden stratospheric warming is difficult to estimate, because the distribution of trace gases is affected by changes in both chemistry (the rates of chemical reactions depend on temperature) and dynamics (changes in wind velocity and mixing between inner and outer vortex air). Recently, Liu et al. (2011) quantified the contributions of both chemistry and dynamics to polar vortex ozone at 24–36 km during the 2002–2003 SSW using measurements by the MIPAS instrument on board the Envisat satellite and the MOZART-3 chemical transport model. The authors have demonstrated a very good agreement between modelled and experimental ozone distributions in the lower and middle stratosphere. The changes at upper altitudes are more difficult for modelling. Simulations with the LIMA model (Sonnemann et al., 2006) have predicted an increase in secondary and tertiary ozone maxima after the occurred temperature minimum in the mesosphere, while the observations (Damiani et al., 2010) have shown more complicated ozone changes.

This paper is dedicated to short-term changes in the middle-atmospheric ozone, $NO_2$ and $NO_3$ distributions caused by sudden stratospheric warmings, as seen by the GOMOS (Global Ozone Monitoring by Occultations of Stars) instrument on board the Envisat satellite. We consider Northern Hemisphere (NH) SSWs in four winters: 2002–2003, 2003–2004, 2005–2006 and 2007–2008. This analysis presents an extension of the previous studies listed above towards a larger altitude range (for ozone, it is 15–100 km), more species (in particular, $NO_3$, which has unique global representation by GOMOS), and a larger number of SSW events (in particular, SSWs in January 2003 and December 2003–January 2004 have not been considered in details in the previous studies). To facilitate analyses, we also use temperature data from MLS (Microwave Limb Sounder) instrument on board the Aura satellite when available, as well as simulations with chemistry-transport models (CTM).

The paper is organized as follows. Brief description of used data and models is presented in Sect. 2. Results and discussion are presented in Sect. 3; they are followed by summary (Sect. 4).

## 2 Data and models

### 2.1 GOMOS measurements of trace gases

GOMOS (Bertaux et al., 2010; Kyrölä et al., 2010b) is the first operational stellar occultation instrument, which measures the stellar spectrum continuously as a star sets behind the Earth limb. Vertical profiles of ozone, $NO_2$, $NO_3$, and aerosol extinction are retrieved from the UV-Visible spectrometer measurements. Since aerosol extinction spectrum is not known a priori, a second-degree polynomial model is used for the description of the aerosol extinction. Due to non-orthogonality of cross-sections of Rayleigh scattering by air with the considered polynomial

model of aerosol extinction, the air density is not retrieved from UV-VIS measurements by GOMOS. It is taken from ECMWF analysis data corresponding to occultation locations. The GOMOS data processing relies on the two-step inversion and a minimal use of a priori information, as described in detail by Kyrölä et al. (1993, 2010b). The vertical resolution (including the smoothing properties of the inversion) of GOMOS ozone profiles is 2 km below 30 km and 3 km above 40 km, and it is ∼4 km for other species. The vertical resolution of the retrieved profiles is the same for all occultations, independent of angles between the orbital plane and the direction to the star, thanks to the "target-resolution" regularization (Kyrölä et al., 2010b; Sofieva et al., 2004; Tamminen et al., 2004). While ozone can be retrieved up to ∼100 km altitude, other species are usually detectable in the upper troposphere and in the stratosphere. Accuracy of the GOMOS retrievals depends on stellar magnitude and spectral class. For this study, we have selected dark-limb occultations (solar zenith angle ≥107° at the tangent point, and ≥90° at the satellite) of hot (effective temperature ≥6000 K) and sufficiently bright (visual magnitude <2.2) stars. The precision of individual ozone profiles is 0.5–2 % in the stratosphere and 1–5 % in the mesosphere and lower thermosphere (MLT), 5–20 % for $NO_2$, and 10–30 % for $NO_3$ (for more details, see Tamminen et al., 2010). The GOMOS night-time data have been extensively compared with collocated ground-based, in situ and satellite data. The main validation results are presented in (Bracher et al., 2005; van Gijsel et al., 2010; Marchand et al., 2004; Meijer et al., 2004; Renard et al., 2008; Verronen et al., 2009, 2005a) .

The spatio-temporal coverage of the selected GOMOS observations related to the sudden stratospheric warmings in the four recent winters is shown in Fig. 1. It is characterized by a very good coverage of northern high latitudes with occultations of very bright stars, which provide a very good precision. The number of occultations for the last two winters is smaller than that available earlier due to the instrumental problems of GOMOS. Latitudes north of 80° N can not be observed after mid-January with sufficiently bright stars. All the considered occultations are in the polar night conditions, except a few days after the 1 February 2008 (see the lines in Fig. 1 indicating the latitude of the polar night terminator).

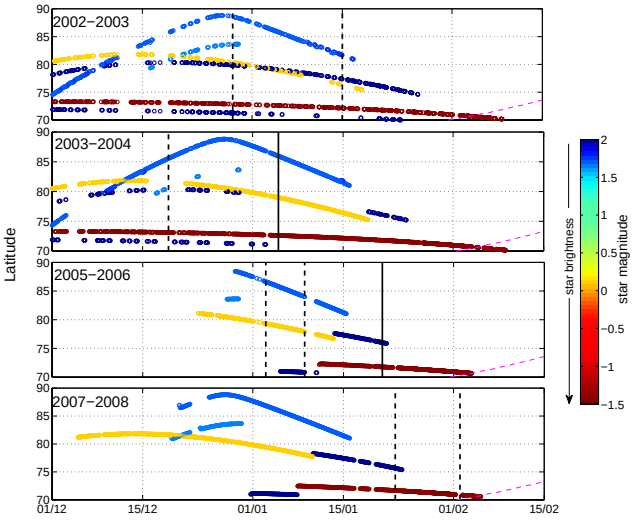


**Fig. 1.** GOMOS data availability in the latitudinal band 70°–90° N in four winters. Colour indicates the visual magnitude of the occulted stars: the smaller the visual magnitude the brighter the star. Black dashed and solid lines indicate onsets of minor and major SSW, respectively. Pink dashed lines indicate the latitude of the polar night terminator.

## 2.2 MLS measurements of temperature

MLS observes thermal microwave limb emission by the atmosphere in five spectral bands from 115 GHz to 2.5 THz (Waters et al., 2006). MLS scans the atmosphere from ground to ∼90 km every 24.7 s, or 240 times per orbit. Scan rate is synchronized to the Aura Orbit, which means that scans are made at the same latitudes each orbit (Fig. 2). The temperature is measured from thermal radiation of $O_2$ using observations near the 118-GHz $O_2$ spectral line. In this paper, temperature profiles v.2.2 are used. They are retrieved using optimal estimation method with GEOS-5 analysis a priori temperature below 1 hPa level and CIRA86 climatology above (Livesey and Snyder, 2004). The vertical resolution of MLS temperature profiles is ∼4 km in the stratosphere degrading down to 8–20 km near the stratopause and in the lower mesosphere; the precisions ranges from 0.6 K in lower stratosphere to 2.5 K in the mesosphere (Schwartz, 2008). Measurements are considered to be valid within the pressure range of 316–0.001 hPa. Comparisons with other previously validated satellite based-measurements show pressure dependent biases of 1–3 K in the lower stratosphere and usually a cold bias of 0–7 K in the mesosphere.

MLS temperature profiles are available from August 2004; they are used for January 2006 and January-February 2008 events. Measurements are performed every 1.5 degrees along the track. The latitudes of the measurements in the band ±82° are essentially the same every orbit, with 30 measurements per day for each latitude. Measurements north of 70° N (Fig. 2) in altitude range 20–80 km were used in this paper, with ∼570 profiles per day in the chosen latitude band.

## 2.3 FinROSE model

FinROSE is a global 3-D offline CTM designed for middle atmospheric studies (Damski et al., 2007). Because the model dynamics (i.e. temperature, horizontal winds and surface pressure) are taken from external sources, the modelled changes in atmospheric composition do not affect the dynamics. In this study FinROSE was run with the

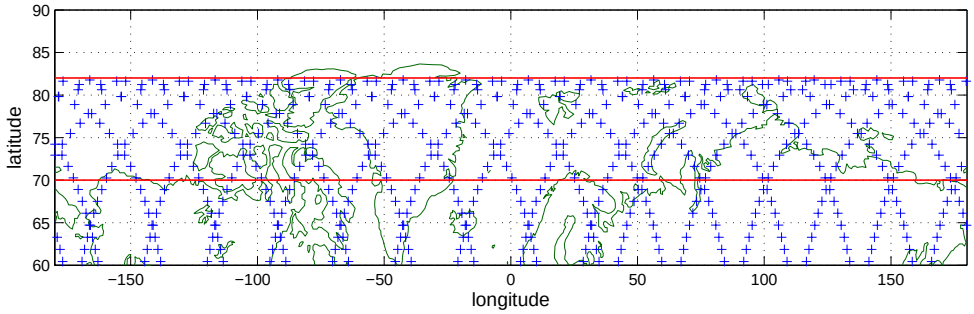


**Fig. 2.** Locations of the MLS profiles for 21 January 2006; red lines indicate the zonal band used in this study.

ECMWF Interim data and with 32 vertical levels from surface up to 0.1 hPa (∼65 km). The horizontal resolution and the number of vertical levels in FinROSE can be modified depending on the resolution of the meteorological data. In this study, the horizontal resolution of 6°(longitude) by 3° (latitude) has been used.

In the model, chemistry is not defined in the troposphere, but the tropospheric abundances are given as boundary conditions. At the lower boundary, monthly averages are used for ozone and water vapour, and trends for long-lived gases. In the stratosphere FinROSE produces distributions of 40 species and families taking into account both chemistry and dynamics. However, only the long-lived constituents are transported. The model includes about 120 homogeneous reactions and 30 photodissociation processes. Chemical kinetic data, reaction rate coefficients and absorption cross-sections are based on the Jet Propulsion Laboratory compilation by (Sander et al., 2006), including updates from the available supplements. The model photodissociation rates are calculated using a radiative transfer model PHODIS (Kylling et al., 1997). In addition, 30 heterogeneous reactions on/in liquid binary aerosols and type Ia, Ib and II polar stratospheric clouds (PSC) are included. The sedimentation of PSC particles, leading to dehydration and denitrification, is also accounted for.

In this study, we used FinROSE model data corresponding to 10:00 p.m., in order to coincide with GOMOS measurements. This means that we get one 3-D field per day and the field is a composite of model results at 10:00 p.m. local time during that day.

### 2.4 SIC model

The Sodankylä Ion and Neutral Chemistry (SIC) model is a one-dimensional tool for studies of middle atmospheric chemistry. SIC was originally developed for interpretation of ionospheric observations (Turunen et al., 1996). The altitude range of the model is 20–150 km, with 1-km resolution. In addition to several hundred ionic reactions, the current version includes neutral reaction schemes of $O_x$, $NO_x$, and $HO_x$, as well as a few other minor constituents (see Verronen et al., 2005b; Verronen, 2006 for a detailed description of SIC). The main external input is solar radiation spectrum, provided by the SOLAR2000 model (Tobiska et al., 2000), which is used to calculate the photoionization and dissociation rates. The model includes a vertical transport scheme, i.e. eddy and molecular diffusion (Banks and Kockarts, 1973; Chabrillat et al., 2002), which affects the vertical distribution of the long-lived species in the mesosphere and lower thermosphere (MLT). In recent years, the model has been used mainly to study the effects of energetic particle precipitation, e.g. solar proton events, in the polar regions and the subsequent interaction between neutral and ionized species (Rodger et al., 2008; Seppälä et al., 2008; Verronen et al., 2008). SIC is focused mainly on the upper atmosphere and it has no heterogeneous chemistry, therefore the SIC data for the polar vortex regions are less robust/reliable below 30 km. In our current paper, SIC was used to study a period of 62 days from 19 December 2005 to 18 February 2006 at two latitudes, 72° N and 77° N. First, the model was initialized to NH winter conditions. Second, periods of 62 days were run using daily average MLS temperature profiles in the reaction rate calculations. Third, a control model run was made, similar to the MLS temperature run except that the 1st day MLS temperature was fixed for the whole duration of the modelling. Because SIC is a 1-D model, it cannot reproduce horizontal transport processes. Also, it cannot be used to study the changes in constituents caused by dynamical changes. Instead, it can provide information on the chemical changes in minor species composition, which are related to the sudden changes in temperature. Therefore, contrasting the SIC results with the changes from observations and the FinROSE 3-D CTM allows us, to some extent, separate the chemical and dynamical effects of the SSW, and discuss their relative importance.

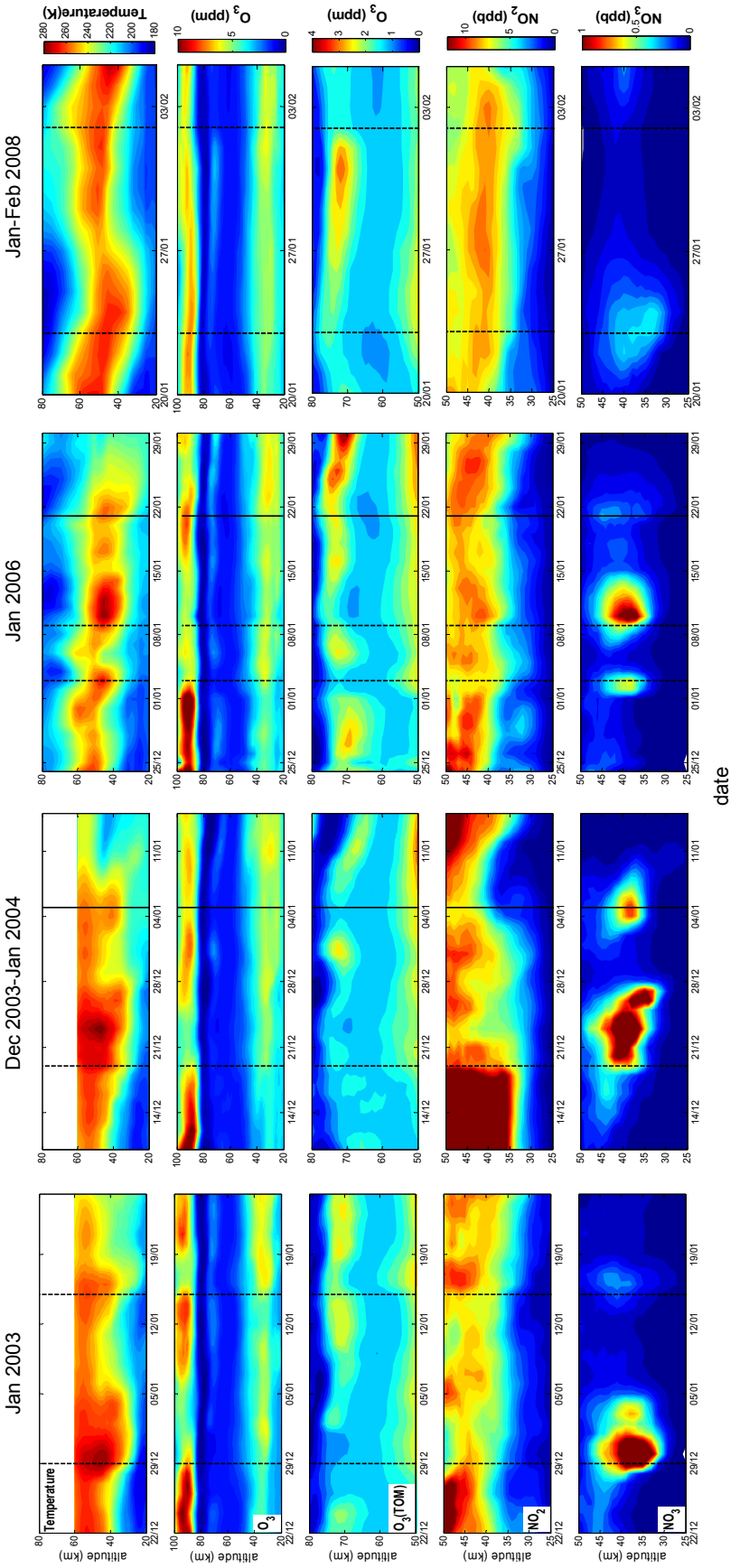


**Fig. 3.** Data at 70°–90° N during four winters; 1st row: temperature from ECMWF (years 2002–2004) and MLS data (years 2006 and 2008); GOMOS observations of ozone (2nd row) with the zoom on tertiary ozone maximum (TOM) (3rd row), $NO_2$ (4th row) and $NO_3$ (5th row). Vertical black dashed and solid lines indicate the onsets of minor and major SSW, respectively.

## 3 Results and discussion

In our analysis, we considered four winters when sudden stratospheric warmings have occurred. We have used the WMO definition of sudden stratospheric warmings: 10 hPa zonal mean winds and temperature gradient reversal poleward of 60° N for more than 5 days (minor SSW) accompanied with zonal mean winds reversal in case of major SSW. In all figures shown in our paper, the onset of a minor SSW (dashed black lines) is the first day of temperature gradient reversal, and the onset of a major SSW (solid black lines) is the first day of zonal wind reversal. In 2008, there were altogether four SSWs (Wang and Alexander, 2009), but only two of them are covered by GOMOS data. The meteorological parameters related to the evolution of polar vortex during these stratospheric warmings are presented e.g. in Kleinböhl et al. (2005); Liu et al. (2009, 2011) for SSW in January 2003, in Liu et al. (2009) for the SSWs in December 2003–January 2004, in Manney et al. (2008); Siskind et al. (2010) for January 2006 SSW, and in Siskind et al. (2010); Wang and Alexander (2009) for the SSWs in 2008. The daily plots of temperature and potential vorticity for SSWs in 2006 and 2008 at several altitude levels can be found at MLS webpage (http://mls.jpl.nasa.gov/data/gallery.php) and at the webpage of high-resolution transport model MIMOSA (Hauchecorne et al., 2002), http://ether.ipsl.jussieu.fr/ether/pubipsl/mimosa_uk.jsp. The evolution of temperature and zonal wind in the stratosphere can be found also at NOAA climate prediction center (http://www.cpc.ncep.noaa.gov/products/stratosphere/strat-trop/).

Figure 3 shows the evolution of temperature and trace gases at 70°–90° N during the four winters. For trace gases, GOMOS observations are used. Temperature is taken from ECMWF analysis (January 2002 and December 2003–January 2004) and MLS (years 2006 and 2008) data. The horizontal distributions and temperature and trace gases at three altitudes (∼40 km, ∼72 km, and ∼95 km) are presented in the Supplement.

For the sudden stratospheric warming of 2006, we run two models: FinROSE CTM (the data at 22:00, the approximate time of GOMOS observations, are shown in Fig. 4 for altitudes 20–65 km) and 1-D chemistry model SIC, which was forced by MLS temperature observations (the evolution of trace gases is shown in Fig. 5). In absence of dynamical mixing in SIC, the concentrations of trace gases (especially $NO_2$ and $NO_3$) depend strongly on latitude, therefore the weighted mean of the simulated data at 72° N and 77° N (with the weights corresponding to the proportion of GOMOS measurements at these latitudes) is presented in Fig. 5. In the following, we discuss the changes in trace gases associated with sudden stratospheric warmings.

### 3.1 Changes in the stratosphere

#### 3.1.1 Introductory notes: stratospheric chemistry in polar night conditions

The distribution of trace gases in the high-latitude winter stratosphere is largely affected by the presence of the polar vortex. The polar night jet acts as a transport barrier between polar and mid-latitude air. Under polar night conditions (absence of solar light), stratospheric $O_x$ species have a long photochemical lifetime, and they are believed to be primarily influenced by transport processes (Brasseur and Solomon, 2005, Fig. 5.11). The ozone loss reaction $O_3 + O \rightarrow 2O_2$ is more effective at higher temperatures (the ozone production is low in the polar night conditions).

Under polar night conditions, ozone destruction in catalytic reaction cycles with halogen compounds (Brasseur and Solomon, 2005) is inactive. Stratospheric ozone is also influenced by reactions with nitrogen oxides, but these are mainly relevant above 30 km and in sunlight conditions. The ozone depletion in the upper stratosphere was clearly observed when amount of $NO_2$ was increased due to solar proton events (SPE) (Seppälä et al., 2004) or strong downward transport of $NO_2$ from the MLT (Hauchecorne et al., 2007; Randall et al., 2006; Renard et al., 2009; Seppälä et al., 2007).

The behaviour of nitrogen compounds in polar regions in winter is the result of complex chemical and physical processes. During night time, NO is rapidly converted into $NO_2$ and further into $NO_3$ by reactions with ozone. $NO_3$ then combines with $NO_2$ to form $N_2O_5$, which provides and important reservoir for nitrogen compounds in the polar winter. $N_2O_5$ can be rapidly converted into nitric acid by the heterogeneous reaction on the surface of sulphate aerosol particles and and/or on the surface of polar stratospheric clouds (the "denitrification" of the lower polar winter stratosphere, Brasseur and Solomon, 2005). For example, the abundance of $NO_x$ is very low inside the Antarctic vortex during winter and spring. Denitrification processes are observed also in the Arctic (e.g., Berthet et al., 2007; Tetard et al., 2009).

In undisturbed conditions (i.e., without SSW), ozone mixing ratio is lower inside the polar vortex than at mid-latitudes in the middle stratosphere (e.g., Kyrölä et al., 2006). Compared to mid-latitudes, night-time $NO_2$ abundances is usually lower inside the polar vortex in the lower stratosphere (see the discussion on denitrification above), but they can be either lower or significantly higher (in case of SPE or strong downward transport from upper altitudes) in the upper stratosphere (e.g. (Hauchecorne et al., 2005), GOMOS global maps at http://fmilimb.fmi.fi/gomosdatapool.html).

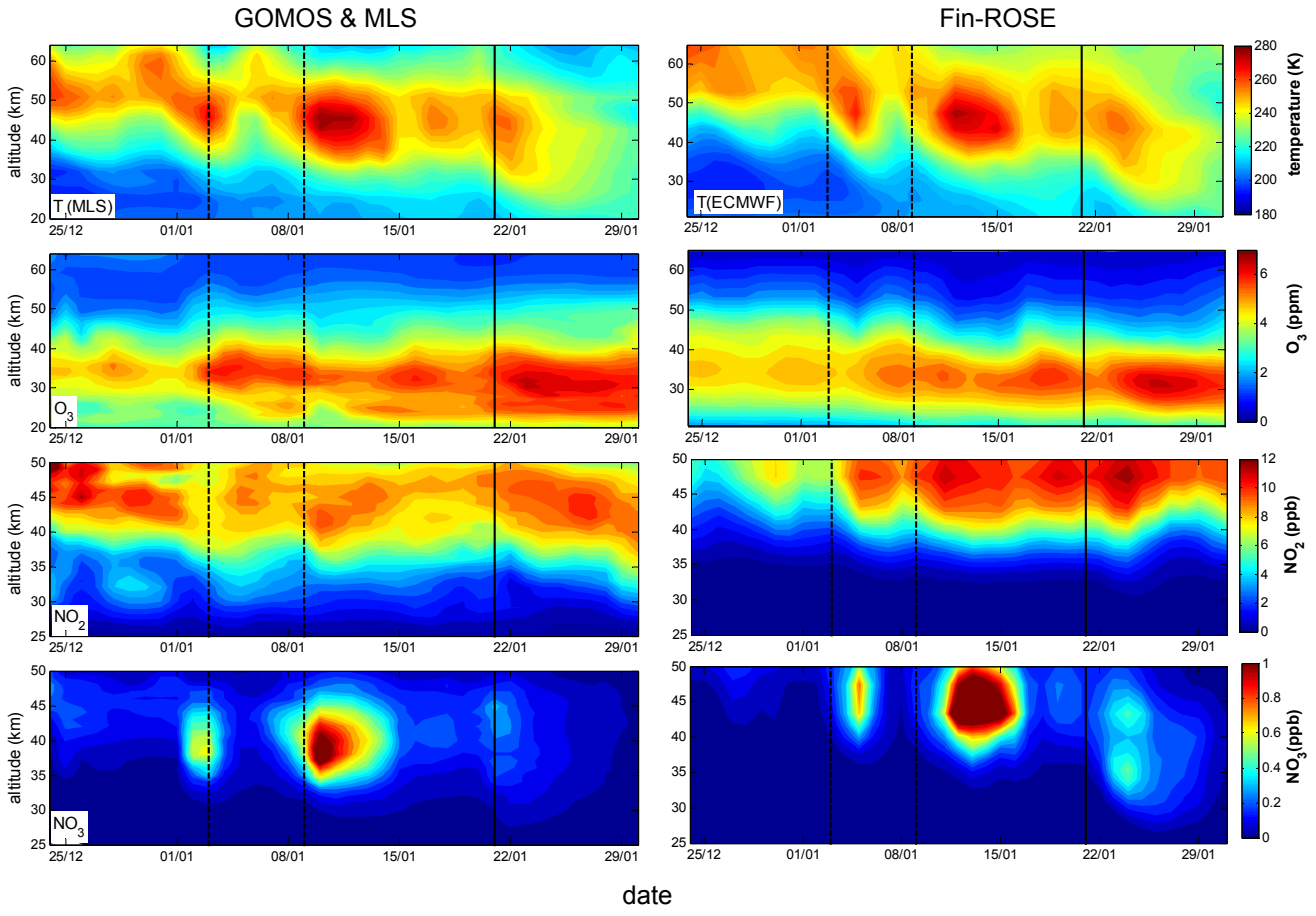


**Fig. 4.** Changes in the middle atmosphere during January 2006 SSW as observed by GOMOS and MLS (left), and as simulated with FinROSE (right). The results present zonally averaged data in the latitudinal band 70°–90° N.

### 3.1.2 Response of stratospheric ozone near the main maximum to SSWs

Since catalytic ozone loss reactions are inactive in the polar night conditions, the response of ozone mixing ratio to SSW is expected to be influenced by the following tendencies: (i) a decrease due to the temperature dependence of ozone loss reaction, (ii) an increase due to mixing with mid-latitude air, and (iii) a decrease with enhancement of vertical transport of ozone-poor air masses from upper altitudes.

Nearly for all considered sudden stratospheric warmings, GOMOS observes a local increase in ozone close to the main stratospheric maximum (Fig. 3). The only exceptions are the major SSW on 5 January 2004 and the minor SSW on 9 January 2006). These ozone enhancements indicate that strong mixing with mid-latitude air is the prevailing reason for the observed changes. The effect of the strong horizontal mixing is revealed also in synchronous $NO_2$ decrease associated with SSWs. This is seen especially clear in SSW on 19 December 2003, which is characterized by high $NO_2$ values before the SSW due to a strong SPE November 2003 (Seppälä et al., 2004). With the onset of this SSW, an ozone enhancement is accompanied with a sharp $NO_2$ decrease as a result of horizontal mixing. These features are also clearly seen on the horizontal maps (Fig. 2 of the Supplement).

The ozone changes for the SSWs in January 2003 are in very good agreement with analyses of Liu et al. (2009) based on MIPAS data. In this work, the authors computed also the ozone budget in the middle-stratosphere polar vortex (24–36 km) using the MOZART-3 CTM. They have shown that ozone change due to horizontal advection dominates over changes due to the vertical advection and due to changed rates of chemical reactions. GOMOS observations confirm these analyses.

For SSWs in 2006, the changes in ozone simulated by FinROSE over the whole considered period are in rather good agreement with GOMOS observations (Fig. 4). However, some differences can be found: for example, GOMOS observes a local increase of ozone associated with SSW on 3 January 2006, while FinROSE ozone is first decreased and then increased. These peculiar differences are

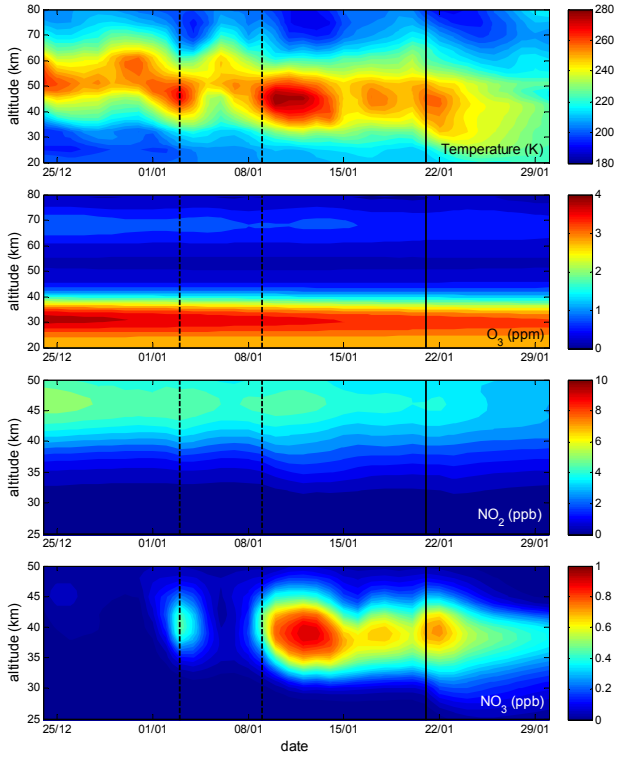


**Fig. 5.** Changes in the middle atmosphere composition during January 2006 SSW as simulated by the SIC model forced by MLS temperature data (shown in the upper panel).

caused probably by the model dynamics (for example, the temperature distributions are slightly different in ECMWF and MLS data) and mixing (see also below).

### 3.1.3 Response of $NO_2$ to SSWs

In polar night conditions, $NO_2$ has a long lifetime, and can be considered therefore as a dynamical tracer. The influence of dynamics (mixing with outside-vortex air) during a SSW may induce a clear enhancement/reduction, if the amount of outside-vortex $NO_2$ is significantly higher/lower than inside.

For $NO_2$, no clear changes associated with onsets of SSW are observed in GOMOS data. Probably, the only exception is minor SSW on 19 December 2003, when a clear decrease in $NO_2$ mixing ratio is observed (this is discussed above). The horizontal maps at ∼40 km (Fig. 2 of the Supplement) show a well-seen anti-correlation between ozone and $NO_2$ distributions for the SSW on 19 December 2003, which indicates their relationship through the catalytic ozone loss reaction.

For SSWs in January 2006, FinROSE predict $NO_2$ enhancements at altitudes 45–50 km, which are well correlated with temperature enhancements at these altitudes (Fig. 4). The similar (but smaller because of smaller values of mixing ratio) changes are observed also in SIC at altitudes 40–50 km (Fig. 5). However, such behaviour is not detected in GOMOS data. In Sect. 3.1.4, we consider quantitative aspects of $NO_2$ response to temperature changes in the whole altitude range 25–50 km and discuss possible reasons for difference between model predictions and observations.

### 3.1.4 Response of $NO_3$ to SSWs

In all GOMOS observations, stratospheric $NO_3$ shows strong enhancements at altitudes 30–45 km during all SSWs. This is clearly observed both in the vertical zonally averaged distributions (Fig. 3), and in the horizontal maps at ∼40 km (Figs. 1–4 of the Supplement). Such behaviour is expected because of strong temperature dependence of the reaction $NO_2+O_3 \rightarrow NO_3$ (Hauchecorne et al., 2005; Marchand et al., 2007). The strong temperature dependence for the $NO_3$ production was first demonstrated by (Renard et al., 2005) using balloon measurements. For the January 2006 SSWs, FinROSE model shows changes in $NO_3$ that are very similar to GOMOS observations. Note that ECMWF temperature, which is used in FinROSE simulations, is different from that observed by MLS during this SSW. Therefore, local enhancements in FinROSE $NO_3$ time series are at slightly higher altitudes and slightly shifted in time with respect to the GOMOS $NO_3$ enhancements (and they correspond to the structure of ECMWF temperature enhancements). For the same event, SIC predicts enhancements in $NO_3$, which are similar to that observed by GOMOS both in magnitude and in altitude location (Fig. 5). However, the SIC $NO_3$ enhancements persist significantly longer than in both GOMOS observations and FinROSE simulations (see enhancement after SSW on 9 January 2006). This indicates that $NO_3$ enhancements associated with SSWs are mostly due to changes in temperature affecting the chemistry, although the higher $NO_3$ values in SIC after 15 January compared to that in GOMOS suggest that dynamical dilution has also an effect.

### 3.1.5 Correlation analysis

To quantify the importance of chemical and dynamical effects in the response of trace gases to sudden stratospheric warmings, we computed correlation coefficients between temperature and trace gases using zonally averaged data at latitudes 70°—90° N from 1 to 25 January 2006, the period of sudden stratospheric warmings. Only short-term changes in the chemical composition associated with SSW events are reflected in this correlation analysis (opposite/complementary to the correlation analysis performed by Damiani et al. (2010) using long time series). Figure 6 shows the correlation coefficient in the altitude range of 20–50 km computed using GOMOS trace gases and MLS temperature observations (left panels), FinROSE (center panels) and SIC (forced by MLS temperature, right panels) simulations.

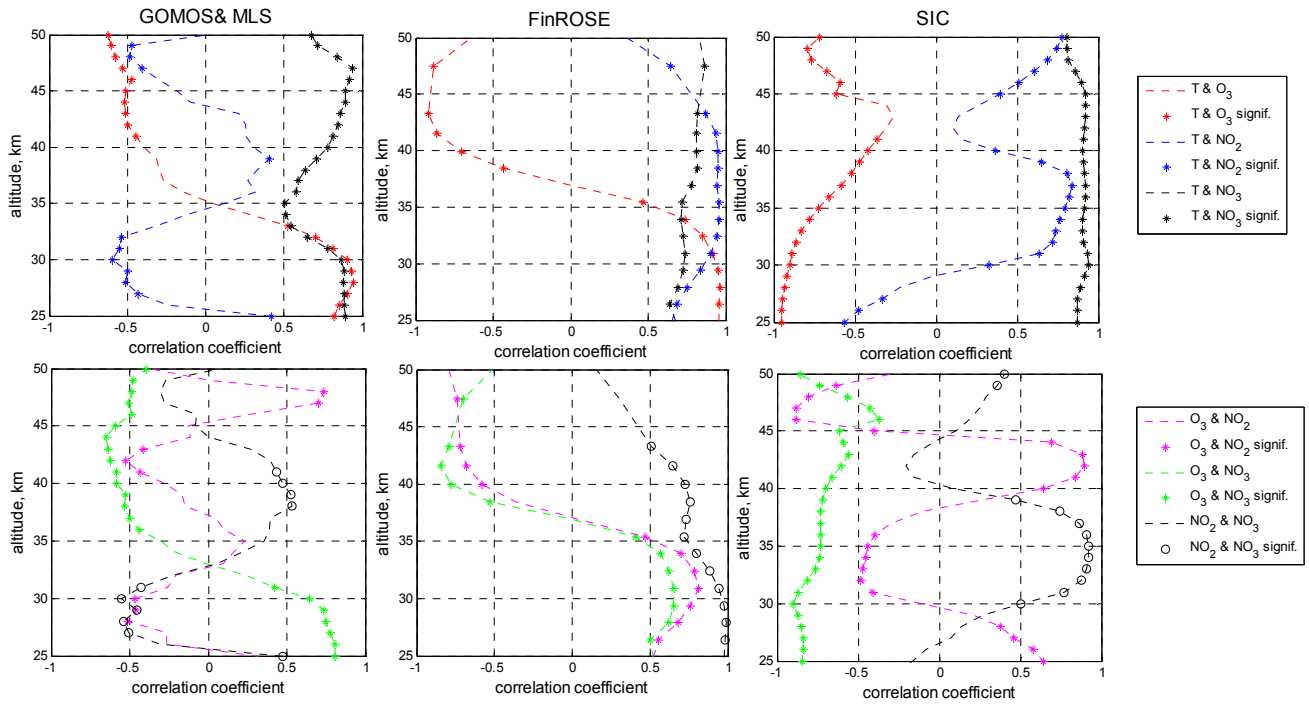


**Fig. 6.** Correlation coefficients between temperature and trace gases using zonally averaged data from 1–25 January 2006 at latitudes 70–90° N; left GOMOS trace gases and MLS temperature, center: FinROSE simulations, right: SIC simulations. Markers (stars and circles) indicate values with statistically significant correlation (i.e., values with probability of zero correlation smaller than 5 %).

As seen in Fig. 6, ozone is correlated with temperature in the dynamically controlled region below ∼35 km, and anti-correlated with temperature at altitudes 35–50 km, where chemical processes dominate. This is observed clearly in both GOMOS and FinROSE data. The SIC model predicts anti-correlation at most altitudes, and a (positive) correlation below 35 km is not even expected, because the absence of dynamics in this model. Note that a similar transition between dynamically and chemically controlled altitude regions has been also observed in previous analyses of sudden stratospheric warmings (e.g., Wang et al., 1983) and in analyses of longer time series at mid-latitudes and in tropics (e.g., Hauchecorne et al., 2010; Kyrölä et al., 2010a). This relationship between stratospheric ozone and temperature has been predicted by theoretical studies and numerical simulations already a long time ago (Rood and Douglass, 1985; Smith, 1995).

As expected and clearly seen in data, $NO_3$ is positively correlated with temperature in the whole altitude range of 25–50 km. The correlation is very high (∼0.9) in SIC simulations (chemistry only), but it is slightly lower when dynamics is taken into account (FinROSE and GOMOS). In GOMOS data, $NO_3$-temperature correlation coefficient has a local minimum at ∼35 km, the altitude of transition from dynamically to chemically controlled altitude regions. A much shallower minimum is also observed in the FinROSE data.

GOMOS $NO_2$ is practically not correlated with MLS temperature data from the considered period. However, a strong correlation between temperature and $NO_2$ is predicted by FinROSE in the altitude range 25–45 km, with some decrease below 30 km and above 40 km. The similar positive correlation between $NO_2$ and temperature was observed also for January 2008 (not shown). In SIC data, a positive significant correlation is observed in January 2005 above 30 km, while the correlation becomes negative below 30 km. These features can be explained by the chemical considerations as follows. In the chemically controlled upper stratosphere, ozone is anti-correlated with temperature. At the same time, ozone is anti-correlated with $NO_2$ through the catalytic ozone loss reaction. These two negative correlations result in positive correlation between $NO_2$ and temperature above ∼35 km. Below 35 km another process seems to dominate: $NO_2$ is positively correlated with temperature through the denitrification of the polar vortex mechanism. The observations indicate favourable conditions for PSC formation before the SSW (e.g., Tetard et al., 2009) and well-seen correlation between $NO_2$ and temperature in the lower stratosphere. FinROSE also shows the presence of PSC before the SSW. In FinROSE, the correlation between

temperature and $NO_2$ is always positive because of the above reasons. In SIC, the temperature-$NO_2$ correlation is positive above ∼35 km, and becomes negative below ∼30 km with the change in temperature-ozone correlation, because SIC does not include the heterogeneous chemistry. The disagreement of GOMOS correlations with that provided by the CTM is probably because the horizontal mixing is underestimated in FinROSE. This assumption is confirmed by considering another SSW in December 2003, when there was a large amount of $NO_2$ in the stratosphere. The realistic amount of $NO_2$ after the Halloween SPE was simulated with FinROSE (see (Funke et al., 2011) for details). Although these pre-SSW $NO_2$ values are comparable to observations, the sharp decrease in $NO_2$with the onset of SSW on 19 December 2003 is not reproduced by FinROSE (not shown here). The correlation between species is more complicated, because it includes implicitly temperature dependence. In particular, significant and nearly constant $O_3$ and $NO_3$ anti-correlation predicted by SIC can be explained by a strong positive temperature-$NO_3$ correlation and a negative temperature-ozone correlation. For the same reason, ozone-$NO_3$ correlation coefficient is positive (and significant) below 30–35 km and negative above 35 km in GOMOS and FinROSE data.

Figure 7 summarizes the experimental correlations between temperature and trace gases by considering all the SSW periods in years 2003, 2004 and 2006. The 2008 SSW is incompletely covered by the GOMOS data and excluded therefore from this analysis. Only statistically significant correlations are shown. They are: strong positive correlation between temperature and $NO_3$, and the significant temperature – ozone correlation changing from positive in the dynamically controlled region below 30–35 km to negative in the chemically controlled region. Ozone-$NO_3$ correlation exhibit a similar sign change due to the two abovementioned correlation. The negative $NO_2$-ozone correlation above 40 km reflects probably their relationship through the catalytic ozone loss reaction.

### 3.2 Secondary ozone maximum

The evolution of the secondary ozone maximum, as observed by GOMOS, during the considered SSWs is shown in Figs. 3 and in 9–12 of the Supplement. According to the GOMOS observations, a clear decrease in secondary ozone maximum is observed practically for all considered SSWs. As seen from the horizontal distributions (Figs. 9–12 in the Supplement), this reduction is observed on the most of the polar cap. The evolution is exceptional/specific for the major SSW on 21 January 2006 and the minor SSW on 23 January 2008. During the minor SSW on 23 January 2008, the secondary maximum has lowered significantly without dramatic changes in the ozone mixing ratio (Fig. 3), therefore the horizontal distribution at altitude ∼95 km (Fig. 12 of the Supplement) shows a significant ozone reduction associated with this SSW. For the major SSW on 21 January 2006 , the variations in secondary ozone maximum are not well aligned with temperature changes in the stratosphere, but they are rather well correlated with the temperature changes in the mesosphere (see also below).

Simulations with SIC and FinROSE models are not available at these altitudes: for FinROSE due to ECMWF data do not extend that high, and for SIC due to large uncertainty of MLS data. The lower-thermospheric ozone is expected to be anti-correlated with temperature and depends on amount of atomic oxygen (production) and hydrogen (destruction) (Smith et al., 2009). On short time-scales, atomic oxygen and temperature are positively correlated, and downward motion increases both. According to (Smith et al., 2009), the chemical lifetime of ozone at the considered latitudes, altitudes and the season is a few minutes. The simulations by Sonnemann et al. (2006) predict increase in the secondary ozone associated with MLT cooling during SSW, while GOMOS data show opposite behaviour. Three of the considered sudden stratospheric warmings: 21 January 2006, 23 January 2008 and 2 February 2008 were observed also with SABER/TIMED instrument; the temperature and ozone changes at these altitudes are reported by Smith et al. (2009). The SABER distributions close to the mesopause exhibit a positive correlation between temperature and ozone associated with SSWs. Specific ozone variations during the 21 January 2006 and 23 January 2008 events are also rather well correlated with corresponding temperature variations (Figs. 1 and 2 in Smith et al., 2009). For these two events, they are shifted in time with respect to temperature changes in the stratosphere.

Based on analysis of SABER temperature, atomic oxygen and ozone in 2002–2009 using longer time intervals, Smith et al. (2009) have pointed out that there is a discrepancy in the current ozone-temperature relationship above ∼90 km (which might be due to incomplete understanding of mesopause ozone or/and due to inconsistent observations). At this stage, GOMOS measurements cannot contribute to resolving this problem, due to the lack of simultaneous observations of O, H, and temperature.

The most probable reason for the observed secondary ozone reduction is a reduced amount of atomic oxygen due to reduced/stopped downward motion with the onset of a SSW. This kind of strong reduction in atomic oxygen was observed in a self-generated SSW by the TIME-GSM/CCM3 model (Liu and Roble, 2002). Quite recent work by Gao et al. (2011), which shows atomic oxygen mixing ratio during SSWs in 2003–2010 retrieved from SABER/TIMED nightglow measurements, has confirmed this hypothesis: a dramatic reduction in atomic oxygen mixing ratio associated with SSWs is observed, up to altitude ∼95 km. Another contributing reason might be the vertical extent of the mesospheric cooling: it might not extend that high, thus a warming might already start at ∼95 km, as shown by Funke et al. (2010). These hypotheses require further elaboration

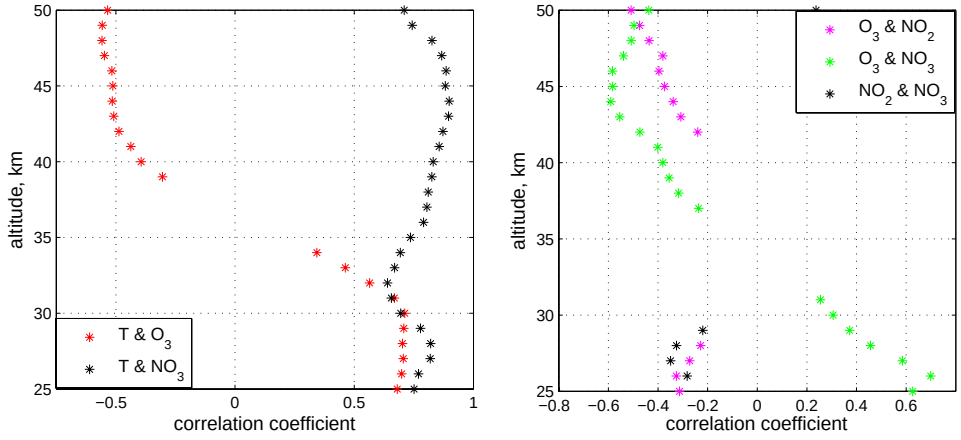


**Fig. 7.** Statistically significant correlations between temperature (MLS and ECMWF) and trace gases (GOMOS) for SSW in years 2003, 2004, and 2006.

using all available experimental data and simulations. Of particular interest can be joint analyses of horizontal and vertical structures. This might be the subject of future work and publications.

### 3.3 Tertiary ozone maximum

The tertiary ozone maximum (TOM) is typically observed in the high-latitude winter mesosphere at altitudes ∼72 km with maximum close to the polar night terminator. It is caused by low concentrations of odd-hydrogen, which result in the subsequent decrease in odd-oxygen losses. Due to a long photochemical lifetime of ozone in the polar night below ∼80 km, TOM can serve as a passive tracer in absence of strong energetic particle precipitation, as shown in Sofieva et al. (2009) and Smith et al. (2009).

Analogously to the secondary ozone maximum, tertiary ozone maximum decreases with the onset of SSW, in some cases, even radically. Such behaviour was observed nearly in all the considered SSWs. Some exceptions – shifts in time with respect to the stratospheric temperature enhancements on zonally averaged evolution plots (Fig. 3) – are observed for 21 January 2006 and 23 January 2008 events (these SSWs are already discussed in connection with the secondary ozone maximum). However, these local variations are well (positively) correlated with temperature variations.

If we consider the response of mesospheric ozone to temperature only, then it is expected to be increased due to a cooling in the mesosphere. This slight increase in TOM can be seen in simulations with 1-D SIC chemical model shown in Fig. 5. At lower latitudes, where there is more sunlight, and in the real atmosphere (taking into account the horizontal mixing), a temperature-induced chemical increase of ozone is expected to be larger. The opposite behaviour of TOM (a reduction instead of an increase) is often observed in GOMOS data. TOM is sensitive to the amount of $HO_x$ species, but, according to (Damiani et al., 2010), OH concentrations do not change much at ∼72 km with the onsets of sudden stratospheric warmings. These are the changes in dynamics accompanied by SSWs that can reduce the tertiary ozone: (i) via horizontal mixing with mid-latitude air or/and (ii) due to the change of the zonal wind from westerly to easterly, which reduces night-time for air parcels and thus the night-time ozone concentration (Doppler-Sonnemann effect, Sonnemann et al., 2006), (iii) reduction of downward transport bringing the dry upper-atmosphere air, and (iv) increased turbulent mixing bringing $HO_x$ from lower latitudes.

The strong horizontal mixing during sudden stratospheric warming occurs also in the mesosphere. It becomes clear when considering the horizontal plots (Figs. 5–8 in the Supplement). The strong horizontal mixing in the mesosphere is well seen also on the maps of tracers (e.g., http://mls.jpl.nasa.gov/data/gallery.php, Fig. 2 in (Seppälä et al., 2007) for SSW on 19 December 2003). When looking at the horizontal maps, interesting features can be noticed for SSWs in January 2003 and January 2004: rather strong TOM enhancements at latitudes ∼60° N at developed stages of the SSWs. Unfortunately, MLS observations are not available for these SSWs. We think that these enhancements can be explained by the changes in the vertical motion associated with stratospheric warmings (phenomena (iii) and (iv) described above).

Overall, we believe that the dynamic processes explain in general the response of TOM to the onset of SSWs. It is worth also to note that the GOMOS observations of tertiary ozone maximum are in good agreement with SABER (Smith et al., 2009) and MLS (Damiani et al., 2010) data for jointly observed SSWs.

## 4 Summary

In this study, we have analyzed GOMOS observations of ozone, $NO_2$ and $NO_3$ during sudden stratospheric warmings in four winters 2002–2003, 2003–2004, 2005–2006 and 2007–2008. As far as we know, the $NO_3$ observations in the stratosphere during SSWs have not been reported before. MLS temperature measurements and simulations with the FinROSE CTM and 1-D ion-chemistry model SIC have been used for analysis and interpretation of changes in the middle atmosphere chemical composition associated with the SSWs. Overall, due to influence of changes in both dynamics and chemical reaction rates, the changes in the trace gases distributions are rather complicated. Our observations and findings can be summarized as follows.

1. Changes in the chemical composition are found not to be restricted to the stratosphere, but they extend to the mesosphere and the lower thermosphere, as expected.

2. Large enhancements of stratospheric $NO_3$, which strongly correlate with temperature enhancements, are observed for all SSWs, as expected by the current understanding of the temperature-dependence of $NO_3$ concentrations and simulations with the CTM.

3. In both experimental data and FinROSE modelling, ozone changes are positively correlated with temperature changes in the lower stratosphere, i.e., in the dynamically controlled region below $\sim$35 km, and they are negatively correlated with temperature in the upper stratosphere (altitudes 35–50 km), where chemical processes are significant.

4. Despite the cooling in the mesosphere and thus expected increase of ozone, the tertiary ozone maximum in the mesosphere often disappears with the onset of SSWs. This can be explained by strong mixing processes.

5. According to GOMOS observations, ozone near the secondary maximum decreases with onset of SSWs almost for all the considered events.

6. The experimental response of $NO_2$ to sudden stratospheric warming exhibits a complicated structure. It seems to be a consequence of strong mixing with outside-vortex air. In particular, if the amount of $NO_2$ inside polar vortex is much higher than outside, a sharp decrease of $NO_2$ with onset of SSWs is observed.

The presented GOMOS observations constitute datasets that are useful for testing 3-D chemistry-transport models, which still exhibit deviations from observations.

**Supplementary material related to this article is available online at: http://www.atmos-chem-phys.net/12/1051/2012/acp-12-1051-2012-supplement.pdf**.

*Acknowledgements.* The authors thank ESA and the GOMOS team for the GOMOS data. This work has been supported by the Academy of Finland projects (MIDAT, SPOC, THERMES) and the ESA Dragon-2 project.

Edited by: W. Ward

## References

Baldwin, M. P. and Dunkerton, T. J.: Stratospheric harbingers of anomalous weather regimes, Nature, 294, 581–584, doi:10.1126/science.1063315 , 2001.

Banks, P. M. and Kockarts, G.: Aeronomy, Academic Press, 355 pp., 1973.

Bertaux, J. L., Kyrölä, E., Fussen, D., Hauchecorne, A., Dalaudier, F., Sofieva, V., Tamminen, J., Vanhellemont, F., Fanton d'Andon, O., Barrot, G., Mangin, A., Blanot, L., Lebrun, J. C., P*é*rot, K., Fehr, T., Saavedra, L., Leppelmeier, G. W., and Fraisse, R.: Global ozone monitoring by occultation of stars: an overview of GOMOS measurements on ENVISAT, Atmos. Chem. Phys., 10, 12091–12148, doi:10.5194/acp-10-12091-2010, 2010.

Berthet, G., Renard, J.-B., Catoire, V., Chartier, M., Robert, C., Huret, N., Coquelet, F., Bourgeois, Q., Rivière, E. D., Barret, B., Lefèvre, F., and Hauchecorne, A.: Remote-sensing measurements in the polar vortex: Comparison to in situ observations and implications for the simultaneous retrievals and analysis of the $NO_2$ and OClO species, J. Geophys. Res., 112, D21310, doi:10.1029/2007JD008699, 2007.

Di Biagio, C., Muscari, G., di Sarra, A., de Zafra, R. L., Eriksen, P., Fiocco, G., Fiorucci, I. and Fuà, D.: Evolution of temperature, $O_3$, CO, and $N_2O$ profiles during the exceptional 2009 Arctic major stratospheric warming as observed by lidar and millimeter-wave spectroscopy at Thule (76.5° N, 68.8° W), Greenland, J. Geophys. Res., 115, D24315, doi:10.1029/2010JD014070, 2010.

Bracher, A., Bovensmann, H., Bramstedt, K., Burrows, J. P., Clarmann, T. V., Eichmann, K.-U., Fischer, H., Funke, B., Gil-López, S., Glatthor, N., Grabowski, U., et al.: Cross comparisons of $O_3$ and $NO_2$ measured by the atmospheric ENVISAT instruments GOMOS, MIPAS, and SCIAMACHY, Adv. Space Res., 36, 855–867, doi:10.1016/j.asr.2005.04.005, 2005.

Brasseur, G. P. and Solomon, S.: Aeronomy of the Middle Atmosphere, 3rd edn., Springer, Dordrecht, 2005.

Chabrillat, S., Kockarts, G., Fonteyn, D. and Brasseur, G.: Impact of molecular diffusion on the $CO_2$ distribution and the temperature in the mesosphere, Geophys. Res. Lett., 29, 1–4, 2002.

Damiani, A., Storini, M., Santee, M. L., and Wang, S.: Variability of the nighttime OH layer and mesospheric ozone at high latitudes

during northern winter: influence of meteorology, Atmos. Chem. Phys., 10, 10291–10303, doi:10.5194/acp-10-10291-2010, 2010.

Damski, J., Thölix, L., Backman, L., Kaurola, J., Taalas, P., Austin, J., Butchart, N., and Kulmala, M.: A chemistry-transport model simulation of middle atmospheric ozone from 1980 to 2019 using coupled chemistry GCM winds and temperatures, Atmos. Chem. Phys., 7, 2165–2181, doi:10.5194/acp-7-2165-2007, 2007.

Dutsch, H. U. and Braun, W.: Daily ozone soundings during two winter months including a sudden stratospheric warming, Geophys. Res. Lett., 7, 785–788, doi:10.1029/GL007i010p00785, 1980.

Flury, T., Hocke, K., Haefele, A., Kömpfer, N., and Lehmann, R.: Ozone depletion, water vapor increase, and PSC generation at midlatitudes by the 2008 major stratospheric warming, J. Geophys. Res., 114, D18302, doi:10.1029/2009JD011940, 2009.

Funke, B., Baumgaertner, A., Calisto, M., Egorova, T., Jackman, C. H., Kieser, J., Krivolutsky, A., López-Puertas, M., Marsh, D. R., Reddmann, T., Rozanov, E., Salmi, S.-M., Sinnhuber, M., Stiller, G. P., Verronen, P. T., Versick, S., von Clarmann, T., Vyushkova, T. Y., Wieters, N., and Wissing, J. M.: Composition changes after the "Halloween" solar proton event: the High Energy Particle Precipitation in the Atmosphere (HEPPA) model versus MIPAS data intercomparison study, Atmos. Chem. Phys., 11, 9089–9139, doi:10.5194/acp-11-9089-2011, 2011.

Funke, B., López-Puertas, M., Gil-Lopez, S., von Clarmann, T., Stiller, G. P., Fischer, H., and Kellmann, S.: Downward transport of upper atmospheric NOx into the polar stratosphere and lower mesosphere during the Antarctic 2003 and Arctic 2002/2003 winters, J. Geophys. Res., 110, D24308, doi:10.1029/2005JD006463, 2005.

Funke, B., López-Puertas, M., Bermejo-Pantaleón, D., Garcia-Comas, M., Stiller, G. P., von Clarmann, T., Kiefer, M. and Linden, A.: Evidence for dynamical coupling from the lower atmosphere to the thermosphere during a major stratospheric warming, Geophys. Res. Lett., 37, L13803, doi:10.1029/2010GL043619, 2010.

Gao, H., Xu, J., Ward, W., and Smith, A. K.: Temporal evolution of nightglow emission responses to SSW events observed by TIMED/SABER, J. Geophys. Res., 116, D19110, doi:10.1029/2011JD015936, 2011.

Garcia, R. R. and Boville, B. A.: "Downward Control" of the mean meridional circulation and temperature distribution of the polar winter stratosphere, J. Atmos. Sci., 51, 2238–2245, 1994.

van Gijsel, J. A. E., Swart, D. P. J., Baray, J.-L., Bencherif, H., Claude, H., Fehr, T., Godin-Beekmann, S., Hansen, G. H., Keckhut, P., Leblanc, T., McDermid, I. S., Meijer, Y. J., Nakane, H., Quel, E. J., Stebel, K., Steinbrecht, W., Strawbridge, K. B., Tatarov, B. I., and Wolfram, E. A.: GOMOS ozone profile validation using ground-based and balloon sonde measurements, Atmos. Chem. Phys., 10, 10473–10488, doi:10.5194/acp-10-10473-2010, 2010.

Glatthor, N., von Clarmann, T., Fischer, H., Funke, B., Grabowski, U., Höpfner, M., Kellmann, S., Kiefer, M., Linden, A., Milz, M., Steck, T., et al.: Mixing Processes during the Antarctic Vortex Split in September–October 2002 as Inferred from Source Gas and Ozone Distributions from ENVISAT–MIPAS, J. Atmos. Sci., 62, 787–800, doi:10.1175/JAS-3332.1, 2005.

Hauchecorne, A., Godin, S., Marchand, M., Heese, B. and Souprayen, C.: Quantification of the transport of chemical constituents from the polar vortex to midlatitudes in the lower stratosphere using the high-resolution advection model MIMOSA and effective diffusivity, J. Geophys. Res., 107, 8289, doi:10.1029/2001JD000491, 2002.

Hauchecorne, A., Bertaux, J.-L., Dalaudier, F., Cot, C., Lebrun, J. C., Bekki, S., Marchand, M., Kyrölä, E., Tamminen, J., Sofieva, V. F., Fussen, D., Vanhellemont, F., D'Andon, O. F., Barrot, G., Mangin, A., Theodore, B., Guirlet, M., Snoeij, P., Koopman, R., de Miguel, L. S., Fraisse, R., and Renard, J. B.: First simultaneous global measurements of nighttime stratospheric $NO_2$ and $NO_3$ observed by Global Ozone Monitoring by Occultation of Stars (GOMOS)/Envisat in 2003, J. Geophys. Res., 110,D18301, doi:10.1029/2004JD005711, 2005.

Hauchecorne, A., Bertaux, J.-L., Dalaudier, F., Russell, J. M., Mlynczak, M. G., Kyrölä, E., and Fussen, D.: Large increase of $NO_2$ in the north polar mesosphere in January–February 2004: Evidence of a dynamical origin from GOMOS/ENVISAT and SABER/TIMED data, Geophys. Res. Lett., 34, 3810, doi:10.1029/2006GL027628, 2007.

Hauchecorne, A., Bertaux, J. L., Dalaudier, F., Keckhut, P., Lemennais, P., Bekki, S., Marchand, M., Lebrun, J. C., Kyrölä, E., Tamminen, J., Sofieva, V., Fussen, D., Vanhellemont, F., Fanton d'Andon, O., Barrot, G., Blanot, L., Fehr, T., and Saavedra de Miguel, L.: Response of tropical stratospheric $O_3$, $NO_2$ and $NO_3$ to the equatorial Quasi-Biennial Oscillation and to temperature as seen from GOMOS/ENVISAT, Atmos. Chem. Phys., 10, 8873–8879, doi:10.5194/acp-10-8873-2010, 2010.

Holton, J. R.: The influence of gravity wave breaking on the general circulation of the middle atmosphere, J. Atmos. Sci., 40, 2497–2507, 1983.

Holton, J. R.: An Introduction to Dynamic Meteorology, 4th edn., Elsevier Academic Press, 2004.

Kleinböhl, A., Kuttippurath, J., Sinnhuber, M., Sinnhuber, B.-M., Küllmann, H., Künzi, K., and Notholt, J.: Rapid meridional transport of tropical airmasses to the Arctic during the major stratospheric warming in January 2003, Atmos. Chem. Phys., 5, 1291–1299, doi:10.5194/acp-5-1291-2005, 2005.

Kylling, A., Albold, A., and Seckmeyer, G.: Transmittance of a cloud is wavelength-dependent in the UV-range: Physical interpretation, Geophys. Res. Lett., 24, 397–400, doi:10.1029/97GL00111, 1997.

Kyrölä, E., Sihvola, E., Kotivuori, Y., Tikka, M., Tuomi, T., and Haario, H.: Inverse Theory for Occultation Measurements, 1: Spectral Inversion, J. Geophys. Res., 98, 7367–7381, 1993.

Kyrölä, E., Tamminen, J., Leppelmeier, G. W., Sofieva, V. F., Hassinen, S., Seppälä, A., Verronen, P. T., Bertaux, J.-L., Hauchecorne, A., Dalaudier, F., Fussen, D., et al.: Nighttime ozone profiles in the stratosphere and mesosphere by the Global Ozone Monitoring by Occultation of Stars on Envisat, J. Geophys. Res., 111, D24306, doi:10.1029/2006JD007193, 2006.

Kyrölä, E., Tamminen, J., Sofieva, V., Bertaux, J. L., Hauchecorne, A., Dalaudier, F., Fussen, D., Vanhellemont, F., Fanton d'Andon, O., Barrot, G., Guirlet, M., Fehr, T., and Saavedra de Miguel, L.: GOMOS $O_3$, $NO_2$, and $NO_3$ observations in 20022008, Atmos. Chem. Phys., 10, 7723–7738, doi:10.5194/acp-10-7723-2010, 2010a.

Kyrölä, E., Tamminen, J., Sofieva, V., Bertaux, J. L., Hauchecorne, A., Dalaudier, F., Fussen, D., Vanhellemont, F., Fanton d'Andon, O., Barrot, G., Guirlet, M., Mangin, A., Blanot, L., Fehr, T.,

Saavedra de Miguel, L., and Fraisse, R.: Retrieval of atmospheric parameters from GOMOS data, Atmos. Chem. Phys., 10, 11881–11903, doi:10.5194/acp-10-11881-2010, 2010b.

Liu, H.-L. and Roble, R. G.: A study of a self-generated stratospheric sudden warming and its mesospheric-lower thermospheric impacts using the coupled TIME-GCM/CCM3, J. Geophys. Res., 107, 4695, doi:10.1029/2001JD001533, 2002.

Liu, Y., Liu, C. X., Wang, H. P., Tie, X. X., Gao, S. T., Kinnison, D., and Brasseur, G.: Atmospheric tracers during the 20032004 stratospheric warming event and impact of ozone intrusions in the troposphere, Atmos. Chem. Phys., 9, 2157–2170, doi:10.5194/acp-9-2157-2009, 2009.

Liu, Y., Liu, C., Tie, X., and Gao, S.: Middle stratospheric polar vortex ozone budget during the warming Arctic winter, 2002–2003, Adv. Atmos. Sci., 28, 985–996, 2011.

Livesey, N. J. and Snyder, W. V.: EOS MLS Retrieval Processes Algorithm Theoretical Basis, Pasadena, California, 2004.

Manney, G. L., Krüger, K., Sabutis, J. L., Sena, S. A., and Pawson, S.: The remarkable 2003–2004 winter and other recent warm winters in the Arctic stratosphere since the late 1990s, J. Geophys. Res., 110(D9), D04107, doi:10.1029/2004JD005367, 2005.

Manney, G. L., Kruger, K., Pawson, S., Minschwaner, K., Schwartz, M. J., Daffer, W. H., Livesey, N. J., Mlynczak, M. G., Remsberg, E. E., Russell III, J. M., and Waters, J. W.: The evolution of the stratopause during the 2006 major warming: Satellite data and assimilated meteorological analyses, J. Geophys. Res., 113, D11115, doi:10.1029/2007JD009097, 2008.

Manney, G. L., Schwartz, M. J., Kruger, K., Santee, M. L., Pawson, S., Lee, J. N., Daffer, W. H., Fuller, R. A., and Livesey, N. J.: Aura Microwave Limb Sounder observations of dynamics and transport during the record-breaking 2009 Arctic stratospheric major warming, Geophys. Res. Lett., 36, L12815, doi:10.1029/2009GL038586, 2009.

Marchand, M., Bekki, S., Hauchecorne, A. and Bertaux, J.-L.: Validation of the self-consistency of GOMOS $NO_3$, $NO_2$ and $O_3$ data using chemical data assimilation, Geophys. Res. Lett., 31, L10107, doi:10.1029/2004GL019631, 2004.

Marchand, M., Bekki, S., Lefèvre, F., and Hauchecorne, A.: Temperature retrieval from stratospheric $O_3$ and $NO_3$ GOMOS data, Geophys. Res. Lett., 34, L24809, doi:10.1029/2007GL030280, 2007.

Matsuno, T.: A dynamical model of the stratospheric sudden warmings, J. Atmos. Sci., 28, 1479–1494, 1971.

Meijer, Y. J., Swart, D. P. J., Allaart, M., Andersen, S. B., Bodeker, G., Boyd, Braathena, G., Calisesia, Y., Claude, H., Dorokhov, V., von der Gathen, P., Gil, M., Godin-Beekmann, S., Goutail, F., Hansen, G., Karpetchko, A., Keckhut, P., Kelder, H. M., Koelemeijer, R., Kois, B., Koopman, R. M. Lambert, J.-C., Leblanc, T., McDermid, I. S., Pal, S., Kopp, G., Schets, H., Stubi, R., Suortti, T., Visconti, G., and Yela, M.: Pole-to-pole validation of ENVISAT/GOMOS ozone profiles using data from ground-based and balloon-sonde measurements, J. Geophys. Res., 109, D23305, doi:10.1029/2004JD004834, 2004.

Randall, C. E., Harvey, V. L., Singleton, C. S., Bernath, P. F., Boone, C. D., and Kozyra, J. U.: Enhanced $NO_x$ in 2006 linked to upper stratospheric Arctic vortex, Geophys. Res. Lett., 33, L18811, doi:10.1029/2006GL027160, 2006.

Randall, C. E., Harvey, V. L., Siskind, D. E., France, J., Bernath, P. F., Boone, C. D., and Walker, K. A.: $NO_x$ descent in the Arctic middle atmosphere in early 2009, Geophys. Res. Lett., 36, L18811, doi:10.1029/2009GL039706, 2009.

Renard, J.-B., Chipperfield, M. P., Berthet, G., Goffinont-Taupin, F., Robert, C., Chartier, M., Roscoe, H., Feng, W., Rivière, E. and Pirre, M.: $NO_3$ Vertical Profile Measurements from Remote Sensing Balloon-Borne Spectrometers and Comparison with Model Calculations, J. Atmos. Chem., 51, 65–78, 2005.

Renard, J.-B., Berthet, G., Brogniez, C., Catoire, V., Fussen, D., Goutail, F., Oelhaf, H., Pommereau, J.-P., Roscoe, H. K., Wetzel, G., Chartier, M., Robert, C., Balois, J.-Y., Verwaerde, C., Auriol, F., Franois, P., Gaubicher, B., and Wursteisen, P.: Validation of GOMOS-Envisat vertical profiles of $O_3$, $NO_2$, $NO_3$, and aerosol extinction using balloon-borne instruments and analysis of the retrievals, J. Geophys. Res., 113, A02302, doi:10.1029/2007JA012345, 2008.

Renard, J.-B., Bekki, S., Blelly, P.-L., Bourgeois, Q., Berthet, G., and Hauchecorne, A.: Analysis of the spatial distribution of the unusual $NO_2$ enhancements in the Arctic polar upper stratosphere and mesosphere observed by GOMOS-Envisat in January–March 2004, J. Geophys. Res., 114, A12323, doi:10.1029/2009JA014174, 2009.

Ricaud, P., Lefèvre, F., Berthet, G., Murtagh, D., Llewellyn, E. J., Mégie, G., Kyrölä, E., Leppelmeier, G. W., Auvinen, H., Boonne, C., Brohede, S., Degenstein, D. A., de La Noë J., Dupuy, E., El Amraoui, L., Eriksson, P., Evans, W. F. J, Frisk, U., Gattinger, R. L., Girod, F. Haley, C. S., Hassinen, S., Hauchecorne, A., Jimenez, C Kyrö E., Lautiè, N., Le Flochmoën, E., Lloyd, N. D., McConnell, J. C., McDade, I. C., Nordh, L. Olberg, M., Pazmino, A., Petelina, S. V., Sandqvist, A., Seppälä, A., Sioris, C. E., Solheim, B. H., Stegman, J., Strong, K., Taalas, P., Urban, J., von Savigny, C., von Scheele, F., and Witt, G.: Polar vortex evolution during the 2002 Antarctic major warming as observed by the Odin satellite, J. Geophys. Res., 110, D05302, doi:10.1029/2004JD005018, 2005.

Richter, A., Wittrock, F., Weber, M., Beirle, S., Kühl, S., Platt, U., Wagner, T., Wilms-Grabe, W., and Burrows, J. P.: GOME Observations of Stratospheric Trace Gas Distributions during the Splitting Vortex Event in the Antarctic Winter of 2002, Part I: Measurements, J. Atmos. Sci., 62, 778–785, doi:10.1175/JAS-3325.1, 2005.

Rodger, C. J., Verronen, P. T., Clilverd, M. A., Seppälä, A. and Turunen, E.: Atmospheric impact of the Carrington event solar protons, J. Geophys. Res., 113, D23302, doi:10.1029/2008JD010702, 2008.

Rood, R. and Douglass, A. R.: Interpretation of Ozone Temperature Correlations 1. Theory, J. Geophys. Res., 90, 5733—5743, 1985.

Salmi, S.-M., Verronen, P. T., Thölix, L., Kyrölä, E., Backman, L., Karpechko, A. Yu., and Seppälä, A.: Mesosphere-to-stratosphere descent of odd nitrogen in FebruaryMarch 2009 after sudden stratospheric warming, Atmos. Chem. Phys., 11, 4645–4655, doi:10.5194/acp-11-4645-2011, 2011.

Sander, S. P., Golden, D. M., Kurylo, M. J., Moortgat, G. K., Wine, P. H., Ravishankara, A. R., Kolb, C. E., Molina, M. J., Finlayson-Pitts, B. J., Huie, R. E., and Orkin, V. L.: Chemical kinetics and photochemical data for use in Atmospheric Studies Evaluation Number 15, JPL, Pasadena, USA., 2006.

Schoeberl, M. R.: Stratospheric warmings: Observations and theory, Rev. Geophys., 16, 521–538, doi:10.1029/RG016i004p00521, 1978.

Schwartz, M. J.: Validation of the Aura Microwave Limb Sounder temperature and geopotential height measurements, J. Geophys. Res., 113, D15S11, doi:10.1029/2007JD008783, 2008.

Seppälä, A., Verronen, P. T., Kyrölä, E., Hassinen, S., Backman, L., Hauchecorne, A., Bertaux, J.-L., and Fussen, D.: Solar Proton Events of October–November 2003: Ozone depletion in the Northern Hemisphere polar winter as seen by GOMOS/Envisat, Geophys. Res. Lett., 31, L19107, doi:10.1029/2004GL021042, 2004.

Seppälä, A., Verronen, P. T., Clilverd, M. A., Randall, C. E., Tamminen, J., Sofieva, V. F., Backman, L., and Kyrölä, E.: Arctic and Antarctic polar winter $NO_x$ and energetic particle precipitation in 2002–2006, Geophys. Res. Lett., 34, L12810, doi:10.1029/2007GL029733, 2007.

Seppälä, A., Clilverd, M. A., Rodger, C. J., Verronen, P. T., and Turunen, E.: The effects of hard-spectra solar proton events on the middle atmosphere, J. Geophys. Res., 113, A11311, doi:10.1029/2008JA013517, 2008.

Siskind, D. E., Eckermann, S. D., McCormack, J. P., Coy, L., Hoppel, K. W. and Baker, N. L.: Case studies of the mesospheric response to recent minor, major, and extended stratospheric warmings, J. Geophys. Res., 115, D00N03, doi:10.1029/2010JD014114, 2010.

Smith, A. K.: Numerical simulation of global variations of temperature, ozone, and trace species in the stratosphere, J. Geophys. Res., 100, 1253–1269, doi:10.1029/94JD02395, 1995.

Smith, A. K., Lopez-Puertas, M., Garcia-Comas, M., and Tukiainen, S.: SABER observations of mesospheric ozone during NH late winter 2002–2009, Geophys. Res. Lett., 36, L23804, doi:10.1029/2009GL040942, 2009.

Sofieva, V. F., Tamminen, J., Haario, H., Kyrölä, E. and Lehtinen, M.: Ozone profile smoothness as a priori information in the inversion from limb measurements, Ann. Geophys., 22, 3411–3420, 2004, http://www.ann-geophys.net/22/3411/2004/.

Sofieva, V. F., Kyrölä, E., Verronen, P. T., eppälä, A., Tamminen, J., Marsh, D. R., Smith, A. K., Bertaux, J.-L., Hauchecorne, A., Dalaudier, F., Fussen, D., Vanhellemont, F., Fanton d'Andon, O., Barrot, G., Guirlet, M., Fehr, T., and Saavedra, L.: Spatio-temporal observations of the tertiary ozone maximum, Atmos. Chem. Phys., 9, 4439–4445, doi:10.5194/acp-9-4439-2009, 2009.

Sonnemann, G. R., Grygalashvyly, M., and Berger, U.: Impact of a stratospheric warming event in January 2001 on the minor constituents in the MLT region calculated on the basis of a new 3-D-model LIMA of the dynamics and chemistry of the middle atmosphere, J. Atmos. Sol.-Terr. Phys., 68, 2012–2025, 2006.

Tamminen, J., Kyrölä, E., and Sofieva, V. F.: Does a priori information improve the retrievals of stellar occultation measurements?, in: Occultations for Probing Atmosphere and Climate – Science from the OPAC-1 Workshop, edited by: Kirchengast, G., Foelsche, U., and Steiner, A. K., 87–98, Springer Verlag, Berlin, Heidelberg, Germany, 2004.

Tamminen, J., Kyrölä, E., Sofieva, V. F., Laine, M., Bertaux, J.-L., Hauchecorne, A., Dalaudier, F., Fussen, D., Vanhellemont, F., Fanton-d'Andon, O., Barrot, G., Mangin, A., Guirlet, M., Blanot, L., Fehr, T., Saavedra de Miguel, L., and Fraisse, R.: GOMOS data characterisation and error estimation, Atmos. Chem. Phys., 10, 9505–9519, doi:10.5194/acp-10-9505-2010, 2010.

Tétard, C., Fussen, D., Bingen, C., Capouillez, N., Dekemper, E., Loodts, N., Mateshvili, N., Vanhellemont, F., Kyrl, E., Tamminen, J., Sofieva, V., Hauchecorne, A., Dalaudier, F., Bertaux, J.-L., Fanton d'Andon, O., Barrot, G., Guirlet, M., Fehr, T., and Saavedra, L.: Simultaneous measurements of OClO, $NO_2$ and $O_3$ in the Arctic polar vortex by the GOMOS instrument, Atmos. Chem. Phys., 9, 7857–7866, doi:10.5194/acp-9-7857-2009, 2009.

Tobiska, W. K., Woods, T., Eparvier, F., Viereck, R., Floyd, L. D. B., Rottman, G., and White, O. R.: The SOLAR2000 empirical solar irradiance model and forecast tool, J. Atmos. Terr. Phys., 62, 1233–1250, 2000.

Turunen, E., Matveinen, H., Tolvanen, J., and Ranta, H.: D-region ion chemistry model, in STEP Handbook of Ionospheric Models, edited by R. W. Schunk, 1–25, SCOSTEP Secretariat, Boulder, Colorado, USA, 1996.

Verronen, P. T.: Ionosphere-Atmosphere Interaction During Solar Proton Events, Finnish Meteorological Institute, Helsinki, Finland, 2006.

Verronen, P. T., Ceccherini, S., Cortesi, U., Kyrölä, E., and Tamminen, J.: Statistical comparison of night-time $NO_2$ observations in 2003-2006 from GOMOS and MIPAS instruments, Adv. Space Res., 43, 1918–1925, doi:10.1016/j.asr.2009.01.027, 2009.

Verronen, P. T., Kyrölä, E., Tamminen, J., Funke, B., Gil-López, S., Kaufmann, M., López-Puertas, M., von Clarmann, T., Stiller, G., Grabowski, U., and Höpfner, M.: A comparison of night-time GOMOS and MIPAS ozone profiles in the stratosphere and mesosphere, Adv. Space Res., 36, 958–966, doi:10.1016/j.asr.2005.04.073, 2005a.

Verronen, P. T., Seppälä, A., Clilverd, M. A., Rodger, C. J., Kyrölä, E., Enell, C.-F., Ulich, T., and Turunen, E.: Diurnal variation of ozone depletion during the October-November 2003 solar proton events, J. Geophys. Res., 110, A09S32, doi:10.1029/2004JA010932, 2005b.

Verronen, P. T., Funke, B., Lopez-Puertas, M., Stiller, G. P., von Clarmann, T., Glatthor, N., Enell, C.-F., Turunen, E., and Tamminen, J.: About the increase of $HNO_3$ in the stratopause region during the Halloween 2003 solar proton event, Geophys. Res. Lett., 35, L20809, doi:10.1029/2008GL035312, 2008.

Wang, L. and Alexander, M. J.: Gravity wave activity during stratospheric sudden warmings in the 2007–2008 Northern Hemisphere winter, J. Geophys. Res., 114, D18108, doi:10.1029/2009JD011867, 2009.

Wang, P.-H., McCormick, M. P., and Chu, W. P.: A study on the planetary wave transport of ozone during the late February 1979 stratospheric warming using the SAGE ozone observation and meteorological information, J. Atmos. Sci., 40, 2419-2431, doi:10.1175/1520-0469(1983)040<2419:ASOTPW>2.0.CO;2, 1983.

Waters, J. W., Froidevaux, L., Harwood, R. S., Jarnot, R. F., Pickett, H. M., Read, W. G., Siegel, P. H., Cofield, R. E., Filipiak, M. J., Flower, D. A., Holden, J. R., Lau, G. K. K., Livesey, N. J., Manney, G. L., Pumphrey, H. C., Santee, M. L., Wu, D. L., Cuddy, D. T., Lay, R. R., Loo, M. S., Perun, V. S., Schwartz, M. J., Stek, P. C., Thurstans, R. P., Boyles, M. A., Chandra, K.

M., Chavez, M. C., Chen, G. S., Chudasama, B. V., Dodge, R., Fuller, R. A., Girard, M. A., Jiang, J. H., Jiang, Y. B., Knosp, B. W., LaBelle, R. C., Lam, J C Lee, K A Miller, D Oswald, J E Patel, N C Pukala, D M Quintero, O Scaff, D. M., Van Snyder, W., Tope, M. C., Wagner, P. A., and Walch, M. J.: The Earth Observing System Microwave Limb Sounder (EOS MLS) on the Aura satellite, IEEE T. Geosci. Remote, 44, 1075–1092, doi:10.1109/TGRS.2006.873771, 2006.